# Effect of $Zn(NO_3)_2$ filler on the dielectric permittivity and electrical modulus of PMMA

**P MAJI[1], P P PANDE[2,\*] and R B CHOUDHARY[1]**

[1]Department of Applied Physics, Indian School of Mines (ISM) Dhanbad, Jharkhand 826 004, India
[2]Department of Applied Sciences, Madan Mohan Malaviya University of Technology, Gorakhpur 273 010, India

**Abstract.** Composite films consisting of polymethyl methacrylate (PMMA) and $Zn(NO_3)_2$ were developed in the laboratory through the sol casting technique. These films were characterized using X-ray diffraction (XRD) and Fourier transform infrared (FTIR) spectroscopy. The morphological analysis was carried out by scanning electron microscopy (SEM). These analyses revealed the homogeneous and semi-crystalline behaviour of the films. The dielectric response measurement was conducted in the frequency range from 100 Hz to 5 MHz. The real and imaginary part of the dielectric permittivity decreased with the increase in frequency but increased with temperature. The electrical conductivity measurement showed a plateau-like behaviour in the low-frequency region and dispersion in the high-frequency region. The frequency-dependent electrical modulus obeyed Arrhenius law, and it showed an increase in the dipolar interaction with the temperature due to thermal activation. The activation energy of the film specimen was estimated to be about 0.448 eV. Thus the polymeric composite $PMMA–Zn(NO_3)_2$ is one of the appropriate candidate for numerous technical applications such as supercapacitors, high-speed computers and gate dielectric material for organic FETs.

**Keywords.** $PMMA–Zn(NO_3)_2$ composite; composite materials; dielectric permittivity; electrical modulus; sol casting.

## 1. Introduction

Organo-inorganic polymeric materials have been popularized globally owing to their outstanding electrical, mechanical and optical properties. These are known to be promising candidates for various applications.[1,2] These hybrid polymeric materials produce multiphase systems with varying physical properties. Further, the synergistic combination of inorganic material or filler with organic polymer is an appropriate step for obtaining novel class of materials with enhanced properties. The polymeric materials are largely multifaceted in comparison to low-molecular-weight compounds. The importance of such materials is well appraised because of the reason that these can be easily manufactured at lower cost. These are flexible and can be processed well at low temperature thereby exhibiting high dielectric break down.[3–6] In an isolated macromolecule, atoms are covalently bonded and linked with a large number of conformations in space and time.[7,8] Due to such conformation, their properties and behaviour are known to be very complex in solution phase.[9] Debye theory of dipolar relaxation apprehends the dielectric spectroscopy greatly for studying the conformation and structure together with the dynamics of polymeric system.[10] The dielectric spectroscopy of polymers provides much more practical information preferably

used for the cable insulation and coating in modern electronic microchips. On the other hand, materials with high dielectric constant and low dielectric loss are needed for the development of high-speed computers. Investigations on dielectric response measurement of polymers and polymeric materials of varying origin have been reported by several researchers especially in high-frequency region.[11] In fact, broad band dielectric spectroscopy beneficiate many advantages owing to the reason that it is capable of monitoring the molecular motion in wide frequency range ($10^{-6}$–$10^{12}$ Hz). Most of the research communications emphasize the usefulness of dielectric spectroscopic study for the better understanding of the phenomenon involved therein. These studies include the dielectric properties of polymer matrix, polymer composites and glassy thermoplastics.[12–16]

Polymethyl methacrylate (PMMA) stands as one of the major categories of functional polymers which have many desirable properties.[17–19] It is the polymeric material that represents numerous physical properties due to its crystal–amorphous interfacial effect.[20] Further, it is a transparent thermoplastic polymer that possesses moderate physical properties. Its dielectric constant is relatively high ($\sim$3–4.9) at room temperature. At the same time, its dielectric loss is also very low over wide frequency range.[21] It is interesting to note that dielectric constant of PMMA is almost invariable with frequency, which makes it a suitable dielectric material for numerous technical applications.[22] Abound[11] conducted an experiment on dielectric spectroscopic study

*Author for correspondence (pppande@gmail.com)

of the PMMA–Cd(NO$_3$)$_2$ composites. His results showed that the real and imaginary part of the dielectric constant increases with the increase in weight percentage of Cd(NO$_3$)$_2$. In the present research communication, we present a study on the effect of Zn(NO$_3$)$_2$ filler in PMMA matrix, with a view to investigate the changes in the dielectric permittivity and electrical properties with the change in temperature and frequency. In the first part of this study X-ray diffraction (XRD), Fourier transform infrared (FTIR) spectroscopy and scanning electron microscopy (SEM) analyses were carried out. In the later part, dielectric properties such as dielectric constant, dielectric loss, ac conductivity and electrical modulus were investigated to study the effect of temperature and frequency on the dipolar motion of the polymeric chain of PMMA–Zn(NO$_3$)$_2$ composite.

## 2. Experimental

### 2.1 *Preparation of PMMA–Zn(NO$_3$)$_2$ composite*

All chemicals used were from Merck Ltd., India. For the preparation of PMMA–Zn(NO$_3$)$_2$ composite, PMMA and Zn(NO$_3$)$_2$ were used as starting materials. The sol casting technique was used to prepare the specimen with the thickness of the order of 220 μm. The PMMA was prepared by free radical polymerization of methyl methacrylate monomer using benzoyl peroxide as initiator. Initially 1.42 g of PMMA was dissolved in 15 ml chloroform. The solution was stirred continuously till a transparent solution was obtained. Further, 0.42 g ZnO (15 nm size) was added to 8 ml of HNO$_3$ and dried in air. The two solutions were added to each other and stirred continuously to get a homogeneous mixture. The solution was transferred into a glass container and allowed to evaporate slowly at atmospheric temperature and pressure. After complete evaporation of the solvent, the specimen was collected in the film form.

### 2.2 *Characterization of PMMA–Zn(NO$_3$)$_2$ composite*

The composite film was characterized using the XRD (Bruker:D-8) technique fitted with advanced Ni-filtered Cu-K$_\alpha$ radiation ($\lambda = 1.5408$ Å). The diffraction patterns were recorded in the angular range 5–90°. The XRD spectra were analysed by comparing the observed peaks with the standard JCPDS data file. The FTIR (Perkin Elmer-RX1) spectroscopic study of pure PMMA, Zn(NO$_3$)$_2$ and PMMA–Zn(NO$_3$)$_2$ composite film was also carried out in the frequency range 400–4000 cm$^{-1}$. The morphological study of the as-prepared PMMA–Zn(NO$_3$)$_2$ composite film was conducted using SEM (ZEISS:SUPRA-55) technique.

### 2.3 *Dielectric evaluation*

The complex dielectric permittivity was investigated using equation $\varepsilon^*(\omega) = \varepsilon'(\omega) - j\varepsilon''(\omega)$; ($\varepsilon'$ is the real part of the permittivity, $\varepsilon''$ the imaginary or loss part with $j = \sqrt{-1}$). The dielectric constant parameters of PMMA–Zn(NO$_3$)$_2$ composite were calculated using equivalent capacitance ($C$), dissipation factor ($D$) as recorded by HIOKI-3250 make LCR meter at a given frequency and temperature. The following set of equations was employed:

$$\varepsilon'(\omega) = c(\omega)\frac{d}{A\varepsilon_0}, \tag{1}$$

$$\varepsilon''(\omega) = \varepsilon'(\omega)\tan\delta, \tag{2}$$

$$\sigma_{ac}(\omega) = \omega\varepsilon_0\varepsilon''(\omega) = \omega\varepsilon_0\varepsilon'(\omega)\tan\delta, \tag{3}$$

where $d$ is the thickness, $A$ the effective area of the specimen, $\sigma_{ac}$ the ac conductivity, $D$ (tan $\delta$) the dissipative factor, $\delta$ the phase angle, $\omega = 2\pi f$, and $f$ the frequency of the applied electric field. Since the complex permittivity is not quite sufficient to describe the electrical property of the polymer composite. Hence, it is desirable to calculate the electric modulus $M^*(\omega)$ of polymeric composite for getting detailed information about its electrical property. This concept was introduced by McCrum *et al*[23] during his research study. According to his research methodology the real and imaginary part of the electric modulus $M^*(\omega)$ can be calculated from $\varepsilon^*(\omega)$ as per the following:

$$M^*(\omega) = \frac{1}{\varepsilon^*(\omega)} = M' + jM'', \tag{4}$$

where the real part of $M^*(\omega)$ follows as

$$M'(\omega) = \frac{\varepsilon'}{\varepsilon'^2 + \varepsilon''^2}. \tag{5}$$

The imaginary part of $M'(\omega)$ follows as

$$M''(\omega) = \frac{\varepsilon''}{\varepsilon'^2 + \varepsilon''^2}. \tag{6}$$

## 3. Results and discussions

### 3.1 *XRD analysis*

For investigating the influence of Zn(NO$_3$)$_2$ content onto the amorphous PMMA polymeric chain, the XRD spectra for pure PMMA, Zn(NO$_3$)$_2$ filler and PMMA–Zn(NO$_3$)$_2$ composite were analysed as shown in figure 1. The XRD pattern of PMMA–Zn(NO$_3$)$_2$ shows a unique characteristics of the composite implying co-existence of mixed crystalline and amorphous region with a strong peak at about 30° (2$\theta$). This reveals the interaction of PMMA polymeric chain with Zn(NO$_3$)$_2$ filler. The addition of filler into the polymeric host changes the intensity and broadness of the existing original peaks. The increase in broadness or reduction in intensity indicates the change (decrease) in the crystallinity of the pristine polymer. The crystallinity of polymer composite film infers the orderly alignment of polymer chains by chain
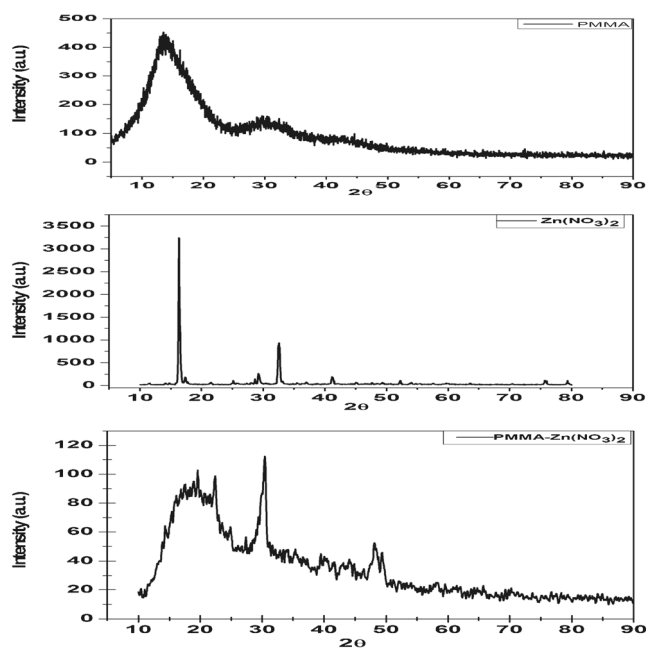
**Figure 1.** XRD spectra for pure PMMA, Zn(NO$_3$)$_2$ and PMMA–Zn(NO$_3$)$_2$ composite.

folding or by the formation of single or multiple helices. This long range order of polymeric chain possesses the degree of crystallinity.[24]

The average crystallites size was calculated by Scherrer's formula[25] as shown below

$$D = \frac{0.9\lambda}{\beta \ \cos \ \theta}, \tag{7}$$

where $\lambda$ is the X-ray wavelength, $\theta$ the angle of Bragg's diffraction and $\beta$ the full-width half-maximum (FWHM). The average crystallites size for the composite was calculated around 40.501 Å. The average chain separation was calculated using the equation as shown below

$$S = \frac{5\lambda}{8 \ \sin \ \theta}, \tag{8}$$

where $S$ is the polymer chain separation, $\lambda$ the wavelength of the XRD and $\theta$ the diffraction angle at the maximum intensity position of the XRD. The average chain separation for PMMA–Zn(NO$_3$)$_2$ composite was estimated around 4.766 Å.

### 3.2 *FTIR analysis*

The molecular structure of the synthesized PMMA–Zn(NO$_3$)$_2$ composite was studied using the FTIR spectroscopic technique. The formation of the polymer composite and the presence of functional groups on the polymer backbone were deduced from the presence of corresponding absorption peak bands in the FTIR spectrum as shown in figure 2. In the high-frequency region two peaks were observed at 3552.39 and 3440.74 cm$^{-1}$, respectively, due to
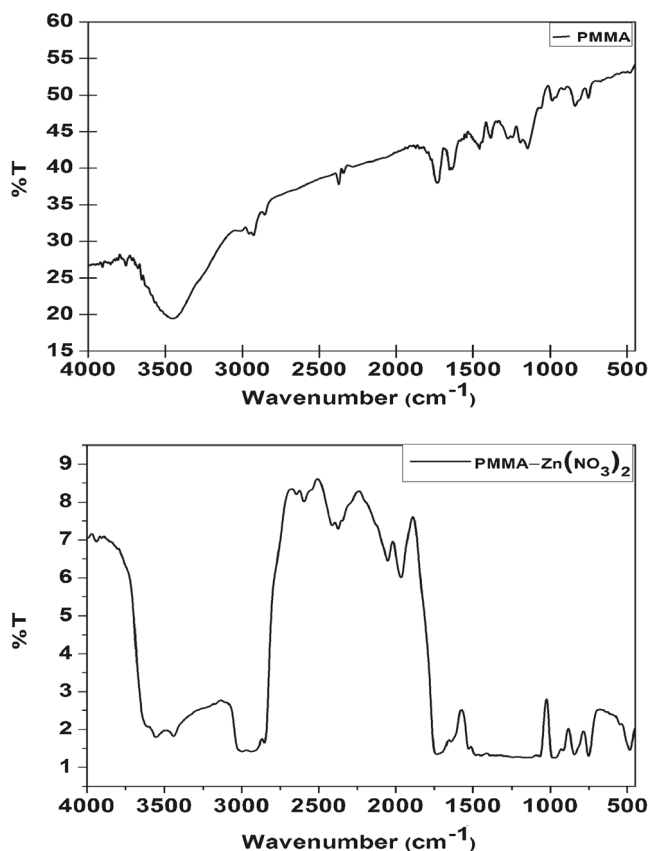


**Figure 2.** FTIR spectra for PMMA and PMMA–Zn(NO$_3$)$_2$ composite.

the N–H stretch. The peaks at 844.67 cm$^{-1}$ was due to NO$_3^-$ bending and the peak at 1731.95 cm$^{-1}$ was due to the C=O stretch of ester. The peaks at 1170.84 and 984.32 cm$^{-1}$ were assigned in plane and out of plane C–H bending.

### 3.3 *SEM analysis*

The morphological study of the PMMA polymer and PMMA–Zn(NO$_3$)$_2$ composite was characterized using scanning electron microscopy (SEM). Figure 3 shows the SEM micrographs of pure PMMA and PMMA–Zn(NO$_3$)$_2$ composite. The average agglomerate size was estimated from SEM image but the actual size of the nanoparticles could not be estimated from SEM image due to the limited resolution of the SEM instrument. The SEM micrograph of PMMA showed the pores and granular morphology of the polymer and the SEM image of PMMA–Zn(NO$_3$)$_2$ confirmed the formation of polymeric composite.

### 3.4 *EDX analysis*

The quantitative and qualitative elemental analyses of the polymeric composite were conducted by making use of energy-dispersive X-ray fluorescence (EDX) spectrometer. This analysis was conducted preferably at the centre of the polymeric composite specimen. The EDX spectra for
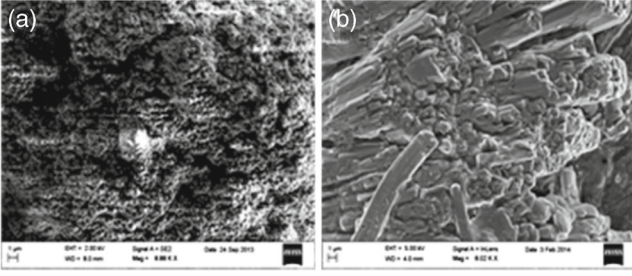
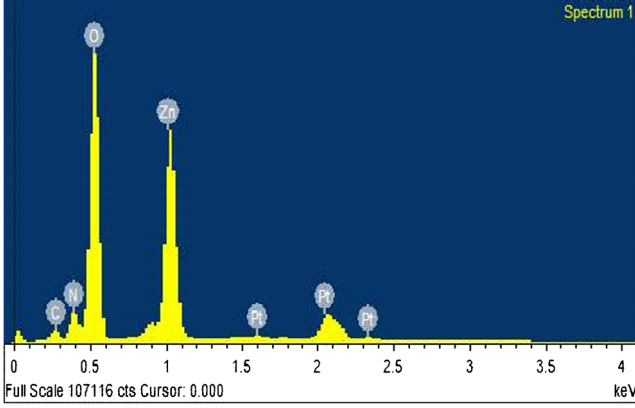**Figure 3.** SEM image for (**a**) pure PMMA and (**b**) PMMA–$Zn(NO_3)_2$ composite.



**Figure 4.** EDX spectra for PMMA–$Zn(NO_3)_2$ composite.

PMMA–$Zn(NO_3)_2$ composite has been shown in figure 4. The spectra represent the respective peaks for the elemental presence of zinc (Zn), nitrogen (N) and oxygen (O) in the PMMA–$Zn(NO_3)_2$ composite along with an auxiliary peak for carbon (C). Additional peak for platinum (Pt) were also observed owing to the surface coating of the specimen with platinum to avoid charging effect. In figure 4, the composition of PMMA–$Zn(NO_3)_2$ composite was analysed and the atomic percentage of Zn, N and O was determined. These were recorded as 13.43, 14.54 and 65.27%, respectively, for Zn, N and O. It was observed that the incorporation of $Zn(NO_3)_2$ in PMMA chain was successfully achieved through the process employed.

### 3.5 *Complex dielectric analysis*

Complex permittivity is a crucial parameter in many RF and MW applications for making reasonably accurate wideband measurements. The dielectric analysis data for polymeric materials and its composite have greater importance when performed in particular frequency ranges. Its precise knowledge is essential for investigating the dielectric feature and related properties. Since the complex dielectric permittivity $\varepsilon^*(\omega)$ is an important factor between an outer alternating electric field $\vec{E}(\omega)$ and resulting polarization ($P$) of the medium.[26,27] It can be shown by the following equation:

$$\vec{P}(\omega) = (\varepsilon^*(\omega) - 1)\varepsilon_0 \vec{E}(\omega), \qquad (9)$$

where $\varepsilon_0 = 8.85 \times 10^{-12}$ F m$^{-1}$ is the permittivity in vacuum, $\omega$ the angular frequency. The measurement data for complex permittivity depends on the physical properties like frequency, temperature, pressure and structure of the materials employed. This is considered as the anisotropic properties of the semi-crystalline polymer or sparsely oriented amorphous polymer. According to statistical mechanics $\varepsilon'$ and $\varepsilon''$ both have significant physical meaning where $\varepsilon'$ stands for the energy stored per cycle and $\varepsilon''$ denotes the energy loss per cycle. There are two different ways to perform dielectric spectroscopic experiment. One is the frequency domain measurement in which experiment is done with sinusoidal alternating field and other is carried out in time domain with a step-like change of electric field to the specimen. In the present study, we performed dielectric measurement in frequency domain. The complex dielectric permittivity related to the free oscillation in an ac electric field as described by Havriliak–Negami relation[28–30] can be shown by the equation

$$\varepsilon^*(\omega) = \varepsilon_\infty + \frac{\varepsilon_S - \varepsilon_\infty}{[1 + (i\omega\tau)^\alpha]^\beta}, \quad 0 \le \alpha, \ \beta \le 1. \qquad (10)$$

Here $\alpha(=1)$ and $\beta(=1)$ are the empirical exponents. This provides the Debye relaxation law, in the case when $\beta = 1$, $\alpha \ne 1$ we get the so-called Cole–Cole (CC) equation in the plot of $\varepsilon''$ *vs.* $\varepsilon'$.[31] The appropriate way to scrutinize the experimental data is to fit with this Cole–Cole expression. Therefore the Debye formula for the frequency-dependent dielectric permittivity has been expressed by the equation

$$\varepsilon^*(\omega) = \varepsilon_\infty + \frac{\varepsilon_S - \varepsilon_\infty}{1 + j\omega\tau}. \qquad (11)$$

The real part of $\varepsilon^*(\omega)$ can be shown as

$$\varepsilon'(\omega) = \varepsilon_\infty + \frac{\varepsilon_S - \varepsilon_\infty}{1 + \omega^2\tau^2}. \qquad (12)$$

And the imaginary part of $\varepsilon^*(\omega)$ can be shown as

$$\varepsilon''(\omega) = (\varepsilon_S - \varepsilon_\infty)\frac{\omega\tau}{1 + \omega^2\tau^2}, \qquad (13)$$

where $\varepsilon_S$ and $\varepsilon_\infty$ are the low and high frequencies values of $\varepsilon^*(\omega)$ with $\omega = 2\pi f$, $f$ is the measuring frequency and $\tau$ the relaxation time. Further the relation between the ac conductivity $\sigma_{ac}$ and complex permittivity $\varepsilon''(\omega)$ can be shown by the equation

$$\sigma_{ac} = \varepsilon_0\omega\varepsilon'', \qquad (14)$$

where $\varepsilon_0$ is the permittivity of the specimen in vacuum, and $\omega$ the frequency.

### 3.6 *Dielectric constant and dielectric loss analysis*

The detailed analysis of dielectric constant and dielectric loss is an important step towards the complete understanding
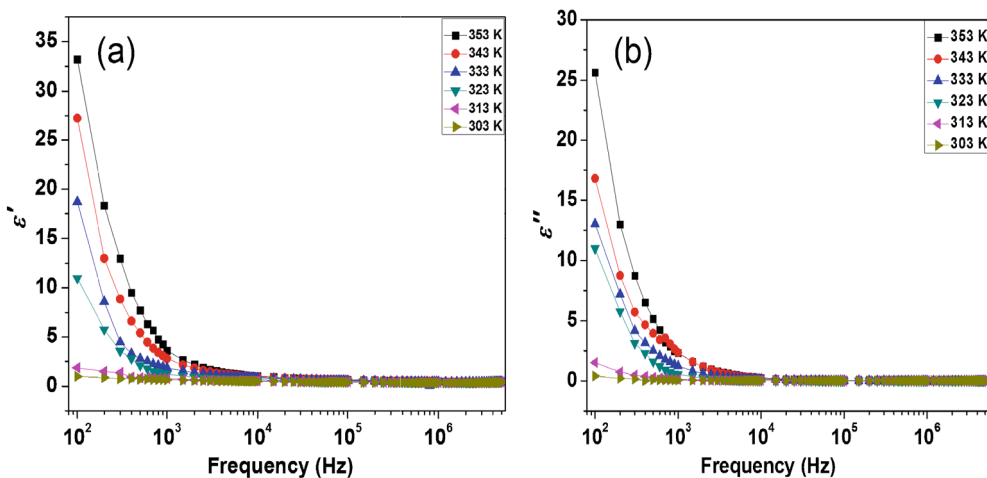
**Figure 5.** Schematic curves for frequency dependent **(a)** $\varepsilon'$ and **(b)** $\varepsilon''$ for PMMA–Zn(NO$_3$)$_2$ composite.

of the dielectric response measurement of the polymeric composite materials. Figure 5a and b shows the frequency-dependent dielectric behaviour of real and imaginary part of the permittivity (dielectric constant and dielectric loss) of the as-prepared PMMA–Zn(NO$_3$)$_2$ composite in the temperature range 303–353 K. Dielectric constant is a function of capacitance, which is proportional to the charge storage on the either surface of the polymeric specimen under an applied electric field.[32] In the high-frequency range (1–5 MHz), the dielectric behaviour of PMMA–Zn(NO$_3$)$_2$ is found to be independent of frequency. It is also observed that in the lower frequency range, dielectric constant and dielectric loss showed non-Debye behaviour, i.e., these increase with the decrease in frequency and increase in temperature.

This occurs due to the reason that the free charge generation takes place at the interface between the polymeric specimen and the electrode (space-charge polarization).[33] If the temperature is close to the glass transition temperature, the charge mobility increases due to improvement in the segmental mobility and hence the permittivity also increases. At the low frequency, space-charge polarization is dominant. However, the higher value of dielectric constant is due to higher grain size as dielectric behaviour depends on the grain size. Since solids are assumed to be composed of grains and grain boundaries. The grains have low resistivity and large thickness where as grain boundaries have high resistivity and small thickness. Due to the contribution of these grain boundaries where impurities reside, the peaks are observed as a result of dielectric loss at low temperature.[34] According to Koop's model, the dielectric constant at lower frequency is observed due to the grain boundaries which possess a high dielectric constant. Further, at high-frequency dielectric constant results from grains which have low dielectric constant.[35] At high frequencies the periodic reversal of electric field is so fast that ions are less capable to diffuse in the field direction. So the polarization decreases due to accumulation of charge.[36] Nonetheless, the dielectric constant also arises due to the frequency-dependent electronic, ionic,
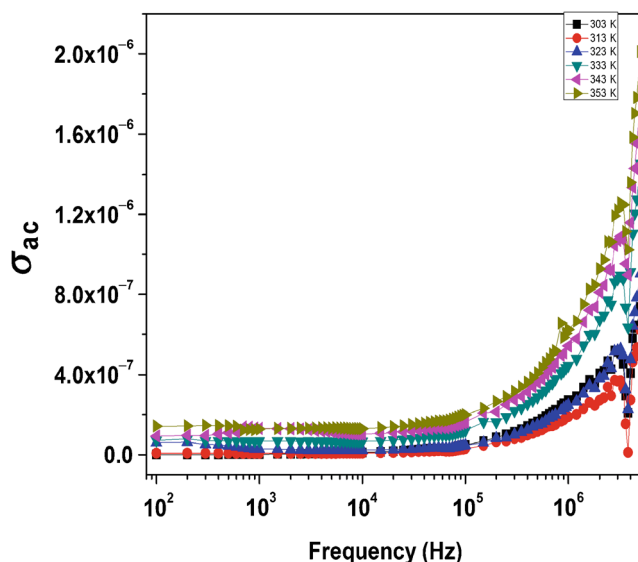


**Figure 6.** Schematic curves for frequency dependence of ac conductivity.

dipolar and surface-charge polarization.[37] As the temperature is increased the dielectric constant is also increased. The reason being, when the temperature is increased, the thermal energy of the molecules and charge mobility also increases. For this reason, the orientational polarization of the specimen increases and the dielectric constant becomes high. At high frequency, the decreasing trend of dielectric constant is not so sharp as compared to low-frequency region. This is due to dipolar orientation which is difficult to rotate at high frequency.

### 3.7 *ac Conductivity analysis*

The ac conductivity of PMMA–Zn(NO$_3$)$_2$ composite were studied and it was found to be a function of frequency as shown in figure 6. The frequency-dependent ac conductivity
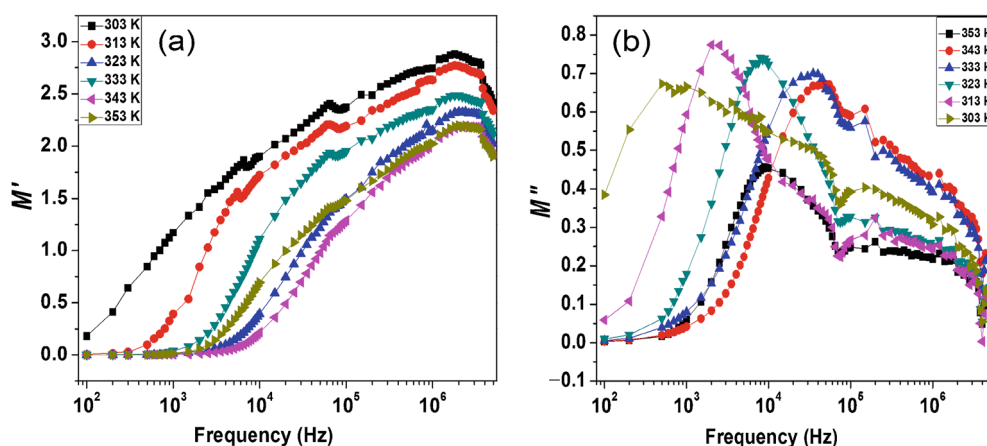
**Figure 7.** Frequency dependent **(a)** $M'$ and **(b)** $M''$ curves for PMMA–Zn(NO$_3$)$_2$ composite.

showed a plateau in the low-frequency region and dispersion at high-frequency region. In the low-frequency region the conductivity is independent of frequency and at high frequency, it is frequency dependent. The early trend in the low-frequency region is due to the free charges available in the polymer matrix and the later one is due to the trapped charges which are only active at high frequency.[38–40] Such a frequency-dependent behaviour may be attributed to the hopping mechanism according to which the electron transport originates from the localized or fixed states within the polymeric chain.

It is also observed that as the temperature increases, the values of ac conductivity increases in the high-frequency range. There are two explanations which exist such that either there is an increase in charge mobility with the temperature as the thermal energy of the molecules increases or there is an increase in charge concentration with the temperature. Since the charge concentration remains almost constant throughout the temperature. Thus the increase in charge mobility may be attributed to the rise in conductivity with temperature. Hence the modification of ac conductive properties of PMMA–Zn(NO$_3$)$_2$ composite films is well observed and appreciated.

### 3.8 *Electrical modulus*

The concept of dielectric permittivity is not sufficiently informative to give an idea about the electrical property of polymer. So an additional concept is required to convert the electrical permittivity in the form of electrical modulus. The electrical modulus is just the reciprocal of complex dielectric permittivity, i.e., $M^*(\omega) = (\varepsilon^*)^{-1}$. Further, the loss spectra are not capable of showing the difference between the interfacial polarization and intrinsic dipolar relaxation. This parameter is very important not only to study interfacial polarization phenomena but also to quantify the molecular dynamics thereof.
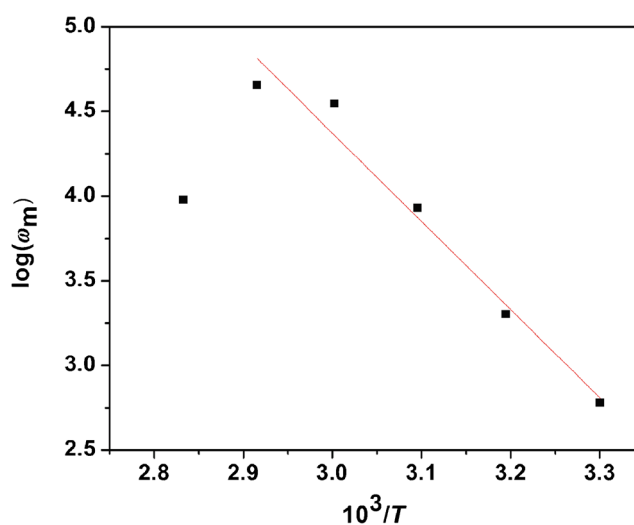


**Figure 8.** Schematic curve for the temperature-dependent probable relaxation frequency.

Figure 7a and b shows the frequency dependence of real ($M'$) and imaginary ($M''$) part of electrical modulus of PMMA–Zn(NO$_3$)$_2$ composite at varying sets of temperature. At high frequency, the $M'$ shows dispersion towards $M_\infty$ (asymptotic value of $M''(\omega)$). At low frequency $M'$ tends to zero value which shows the low contribution of electrode polarization to $M'$. Here the polarization occurs at the interface of the polymer matrix and the inorganic filler Zn(NO$_3$)$_2$. In the frequency-dependent $M''$ plot, a peak is observed which is shifted to high-frequency region as the temperature increases. This peak is observed due to the imperfections within the crystalline phase. The chain rotation and twisting within the interior of the crystals discontinues the defects.[21,41–43] As the temperature increases, there is an increase of dipole mobility, i.e., charge mobility is activated thermally and the hopping mechanism takes place. Here $f_{max}$ is the characteristic frequency and define the relaxation time by $2\pi f_{max} = 1$ which is a measure of characteristic time $\tau$.[34]

The characteristic time of the interfacial polarization obeys the Arrhenius law as shown below

$$\omega_m = \omega_0 \exp\left[\frac{-E_a}{k_\beta T}\right], \tag{15}$$

where $\omega_0$ is the pre-exponential factor, $k_\beta = 1.38 \times 10^{-23}$ J K$^{-1}$ the Boltzmann constant, $T$ the absolute temperature and $E_a$ the activation energy. Figure 8 shows the schematic curves for log $\omega_m \sim 1/T$. The activation energy thus calculated is around 0.448 eV.

## 4. Conclusions

The polymeric composite of PMMA–Zn(NO$_3$)$_2$ was successfully prepared by the addition of Zn(NO$_3$)$_2$ filler into PMMA polymer. The XRD and FTIR data revealed the incorporation of inorganic filler into the polymer chain. The analysis of the dielectric permittivity and ac conductivity of the composite revealed that the addition of inorganic filler Zn(NO$_3$)$_2$ enhanced the dielectric behaviour of PMMA polymer. The dielectric analysis showed that at low frequency, the relative permittivity sharply decreased with the increase in frequency. However at high frequency, it showed frequency-independent behaviour. This can be explained on the basis of the phenomena of space charge polarization. Further, the ac conductivity showed a plateau in the low-frequency region and dispersion at the high-frequency region. The increase in ac conductivity was due to the creation of additional hopping sites in the polymeric composite. Thus the frequency-dependent ac conductivity could be attributed to the hopping mechanism. The frequency-dependent electrical modulus curves obeyed the Arrhenius law. The activation energy as calculated from the Arrhenius law was found around 0.448 eV. It was also observed that as the temperature increases, the dipole mobility also increases, resulting into the increase in the dipolar interaction. Thus the polymeric composite PMMA–Zn(NO$_3$)$_2$ is one of the appropriate candidate for numerous technical applications such as supercapacitors, high-speed computers and gate dielectric material for organic FETs.

## Acknowledgement

## References

1. Ajayan P M, Schadler L S and Braun P V 2003 *Nanocomposite science and technology* (Wiley: New York) p. 112

2. Jordan J, Jacob K I, Tannenbaum R, Sharaf M A and Jasiuk I 2005 *Mater. Sci. Eng. A* **393** 1

3. Jin Z, Pramoda K P, Xu G and Goh S H 2001 *Chem. Phys. Lett.* **337** 43

4. Isojima T, Suh S K, Sande J B V and Hatton T A 2009 *Langmuir* **25** 8292

5. Kim H, Daniels E S, Dimonie V L and Klein A 2009 *J. Appl. Polym. Sci.* **112** 843

6. Koh H, Changez M and Lee J 2009 *Macromol. Rapid Commun.* **30** 1583

7. Flory P J 1988 *Statistical mechanics of chain molecules* (Munich Vienna, New York: Hanser Publishers)

8. Wolkenstein M V 1963 *Configurational statistics of polymeric chains* (New York: Wiley Inter-science)

9. Schönhals A 1987 *Bundesanstalt für Materialforschung und-prüfung, Fachgruppe VI 3.2* (Berlin, Germany: Unter den Eichen) p. 12205

10. Debye P 1945 *Polar molecules* (New York: Chemical Catalog Co., reprinted by Dover Publisher)

11. Abound L H 2013 *Nat. Appl. Sci.* **4** 73

12. Santos S, Cedeño A and Gómez C 1999 *Polym. Eng. Sci.* **39** 1752

13. Perusich S and Brearty M C 2000 *Polym. Eng. Sci.* **40** 214

14. Dabek R 1996 *Polym. Eng. Sci.* **36** 1065

15. Steeman P A M, Maurer F H J and Turnhout J V 1994 *Polym. Eng. Sci.* **34** 697

16. Chen M, Siochi E J, Ward T C and McGrath J E 1993 *Polym. Eng. Sci.* **33** 1110

17. Ramesh S and Wen L C 2010 *Ionics* **16** 255

18. Yap K S, Teo L P, Sim L N, Majid S R and Arof A K 2012 *Physica B* **407** 2421

19. Demir M M, Koynov K, Akbey U, Bubeck C, Park I, Lieberwirth I and Wegner G 2007 *Macromolecules* **40** 1089

20. Abdelaziz M and Abdelrazek E M 2007 *Physica B* **390** 1

21. Namouchi F, Smaoui H, Fourati N, Zerrouki C, Guermazi H and Bonnet J J 2009 *J. Alloys Compd.* **469** 197

22. Kumar S, Rath T, Khatua B B, Dhibar A K and Das C K 2009 *J. Nanosci. Nanotechnol.* **9** 4644

23. McCrum N G, Read B E and Williams G 1967 *Anelastic and dielectric effects in polymeric solids* (London: Wiley)

24. Smyrl W H, Lien M and Scrosati 1993 *Applications of electroactive polymers* (London: Chapman and Hall)

25. Cullity B D 1978 *Element of X-ray diffraction* (London: Anderson-Wesley)

26. Böttcher C J F and Bordewijk P 1973 *Theory of dielectric polarization* (Amsterdam: Elsevier)

27. Cook M, Watts D C and Williams G 1970 *Trans. Faraday Soc.* **66** 2503

28. Hill N E, Vaughan W E, Price A H and Davis M 1969 *Dielectric properties and molecular behaviour* (London: Van Nostrand)

29. Böttcher C F and Scaife P 1989 *Principles of dielectrics* (Oxford: Oxford University Press)

30. Havriliak S and Negami S 1966 *J. Polym. Sci. Part C* **14** 99

31. Davidson D W and Cole R H 1951 *J. Chem. Phys.* **19** 1484

32. Dang Z M, Zhang Y H and Tjong S C 2004 *Synth. Met.* **146** 79

33. Roy D K, Himanshu A K and Sinha T P 2007 *Indian J. Pure Appl. Phys.* **45** 692

34. Sattar A A and Rahman S A 2003 *Phys. Status Solidi (A)* **2** 415

35. Koops C 1953 *Phys. Rev.* **83** 121

36. Latif F, Aziz M, Katun N, Ali M and Yahya M Z A 2006 *J. Power Sources* **1594** 1401

37. Fang S, Ye C H, Xie T, Wong Z Y, Zhao J W and Zhang L D 2006 *Appl. Phys. Lett.* **88** 013101

38. de Oliveira H P, dos Santos M V B, dos Santos C G and de Melo C P 2003 *Mater. Charact.* **50** 223

39. de Oliveira H P, dos Santos M V B, dos Santos C G and de Melo C P 2003 *Synth. Met.* **135** 447

40. Macedo P B, Moynihan C T and Bose R 1972 *Phys. Chem. Glasses* **13** 171

41. Nakagawa K and Ishida Y 1973 *J. Polym. Sci.: Pol. Phys.* **11** 2153

42. Mijovic J, Sy J W and Kwei T K 1997 *Macromolecules* **30** 3042

43. Arous M, Ben Amor I, Kallel A, Fakhfakh Z and Perrier G 2007 *J. Phys. Chem. Solids* **68** 1405